

## FRAMEWORK FOR FDG-PET AND MRI FOR AUTOMATED EXTRASKELETAL BONE SARCOMA WITH CANCER DETECTION

Baskaran<sup>1</sup>, Malathi<sup>2</sup>, Thirusakthimurugan<sup>3</sup><sup>1</sup>\* Dept. of ECE/DrPEC and Research Scholar, Annamalai University, INDIA<sup>2</sup> Dept. of EIE, Annamalai University, Chidambaram, INDIA<sup>3</sup>Dept. of EIE, Pondicherry Engineering College, Pondicherry, INDIA

## ABSTRACT

Soft Tissue Sarcoma (STS) is a heterogeneous set of connective tissue malignancies that emerge from tissues of mesenchymal origin. They comprise lesser than 1% of all adult malignancies. Morphologic imaging modalities like CTs as well as MRIs may be utilized for assessing tumour localizations, size as well as infiltrations of the surrounding tissues and presence of stellate metastases. FDG PET imaging is complementary to radiological tomography as well as histological grading. Features are extracted through Wavelets as well as Wavelet and Grey Level Co-occurrence Matrix (GLCM). Correlation-based features selection methods are utilized for features selection. Structural optimization is suggested through usage of binary particle swarm optimization for classification. Neural networks are utilized as classifiers. Experimental evaluation confirmed the efficacy of the suggested technique

Published on: 14<sup>th</sup>– August-2016

## KEY WORDS

Soft Tissue Sarcoma (STS),  
Grey Level Co-occurrence  
Matrix (GLCM), Wavelets,  
Neural Networks, Levenberg  
Marquardt

\*Corresponding author: Email: [baskaranpec@gmail.com](mailto:baskaranpec@gmail.com); [vsmalu@gmail.com](mailto:vsmalu@gmail.com), [thirusakthimurugan@pec.edu](mailto:thirusakthimurugan@pec.edu)

## INTRODUCTION

Sarcoma refers to a heterogeneous set of tumours which emerge from tissues of mesenchymal origin. They are a rare kind of tumours and make up only around 1.5% of all cancers. Classifications by the World Health Organization (WHO) pinpoint around fifty distinct subkinds. Molecular study has revealed that the various subkinds are in fact biologically different which implies that sarcomas are basically a set of very rare diseases, more so than others. Clinically speaking, sarcomas are split into soft-tissue sarcomas (STS), bone sarcomas, and gastrointestinal stromal tumours (GIST) [1]. STS represents both the biggest as well as most heterogeneous set of tumours amongst sarcomas. Sarcoma originates basically from elements in the mesodermal embryonic layers. [2].

F-fluorodeoxyglucose positron emission tomography (FDG PET) is capable of identifying primary, recurrent as well as metastatic cancers in the breasts, colon, lungs as well as lymphoma in a successful manner. It is also capable of detecting STS as well as providing an indicator of grade. There is very little data available on its usage in earlier detection of local recurrence and metastases after primary surgical treatment of soft-tissue sarcomas. FDG-PET also has the benefit of detecting both problems in one procedure. Two individuals had whole-body FDG-PET initially during the evaluation stage and were hence incorporated only in the assessment of the value of FDG PET in the identification of distant metastases.

FDG-PET/CT both refer to imaging tools which are capable of measuring a tumour's metabolic activity and might be more helpful than Response Evaluation Criteria in Solid Tumors (RECIST) for the assessment of the efficacy of therapy as well as the prediction of survival of the afflicted individual. The tool exploits the fact that aggressive tumours utilize great levels of glucose for fuelling their growth and utilize radio-labelled glucose for measuring tumour's metabolic activities. Although FDG-PET/CT scans are now a fundamental part of cancer follow-up care, two UCLA works offer proof that the scans are efficient for direction of treatment schemes earlier in the care of the patients. FDG-PET/CT is capable of detecting the stage of sarcoma in children and research is being conducted to observe if it is capable of determining earlier response to therapies like in the case of adults [3].

Contrast improved Magnetic Resonance Images (MRI) displayed a  $5.1 \times 4.2 \times 11.0$  cm multilobulated forearm mass with prominent peripheral improvement as well as a central non-improving element. The mass was centred at the flexor digitorum profundus and did not appear to be involved with the base osseous structure. FDG PET scans were consequently obtained. Mild, diffused as well as increased activities all through the muscles secondary to insulin administration was present. Administration of insulin was carried out for lowering serum glucose to large right forearm soft tissue masses or within several lung nodules. The individual was chemoradiotherapy naïve when PET scan was taken [4]. Follow-up MRIs of upper extremities revealed extreme distribution of tumours by original extensions and it also infiltrated into the axilla, scapular musculature as well as underlying rib cage. CT scans of the chest revealed that there was considerable worsening of pulmonary as well as parenchymal metastatic diseases.

Hence, it is considerably significant to detect individuals who will potentially have benefits from chemotherapies or other molecule targeted agents. Morphological imaging modalities such as CTs or MRIs may be utilized for assessing tumour localization, size as well as infiltration of the surrounding tissue apart from the presence of satellite metastases. But it is not conclusively proved that considerable changes in the size of tumours are a useful tool of result of individuals suffering from soft-tissue sarcoma. Standard radiographic responses have not correlated in a consistent manner with histological responses or with illness-free survival. Other techniques for identifying individuals who will probably find chemotherapy or other agents beneficial would be of great use. Hence, PET with F-FDG is increasingly finding great usage in oncology as it permits functional imaging of viable tumorous tissue. But not every tumour is PET avidin spite of being viable.

Structural optimization is proposed through usage of binary particle swarm optimization for the classification. The remaining sections organized as: Section 2 presents the related work in literature. Section 3 details the methods which are utilized in the proposal. Section 4 discusses the experiment results and section 5 gives the conclusion of the proposed work.

## LITERATURE REVIEWS

Farhidzadehet al., [5] suggested a new model for the classification of STSs that had a focus on radiologically-defined sub-areas known as habitats. The important habitats are areas wherein the evolution of tumours can be seen. The investigators measured T1 post- as well as pre-contrast gadolinium as well as T2 non-contrast MRIs of 36 patients before treatment. The suggested method took into consideration spatially separate habitats that might be useful in clinical treatments, particularly chemotherapy as well as radiation.

Karakatsanis et al., [6] suggested the facilitation of transitions from static to dynamic multi-bed FDG PET/CT imaging wherein considering the trouble of sparse temporal sampling at all beds, new dynamic acquisition strategies are to be utilized for yielding quantitative whole-body imaging of FDG uptakes. A group of new dynamic multi-bed PET images acquisition strategies have been formulated through usage of Monte Carlo simulation, for quantitative evaluations of the clinical feasibility of the technique as well as optimization of the quantity of passes per bed as well as the total study time period. In the end, clinical whole-body patient information has been obtained in a dynamic manner and the outcomes revealed the potential of the suggested technique in the enhancement of treatment response monitoring capacities of clinical PETs researched.

O'Sullivan et al., [7] presented new methods of characterizing the total profile of the tumours, as well as a method for measuring the phase of development. Phase metric is capable of distinguishing between the earlier phase tumours wherein uptake is greatest at the core and latter phase masses wherein frequently there may be central voids in FDG uptakes. A set of FDG-PETs examined from around 185 individuals is utilized for the formal evaluation of the prognostic benefits. The study proved that more detailed quantitative appraisals of the spatial patterns of PET image data of tumour masses, beyond the maximal FDG uptakes (SUVmax) as well as earlier regarded metrics of heterogeneity, offer enhanced data for possible inputs to treatment decisions for future cases.

Wanget al., [8] suggested an automatic protocol for the detection of occurrences as well as changes of hotspots in intra-subject FDG-PET scans from fused PET-CT scanners. In this protocol, several CT scans of one subject were aligned through the usage of affine transformations, while the predicted transformations are then utilized for aligning the related PET scans into the same coordinate systems. Hotspots were detected through thresholding as

well as regions growing with variables defined particularly for various body parts. The alterations of the identified hotspots with time are examined and provided. The outcomes in nineteen clinical PET-CT studies proved that the suggested method yielded excellent performance.

Zhong and Kundu [9] suggested an optimized compartment framework that is capable of concurrently correcting for spillovers as well as partial volume impacts for both blood as well as tissue, calculate kinetic rate variables as well as create model corrected blood input functions (MCBIF) from OS EM-MAP cardio-respiratory gated <sup>18</sup>F-FDG PET scans of mouse heart with attenuation corrections in vivo, with no invasive blood sampling. The method improves quantitation however it is iterative.

Mabrouk et al., [10] obtained rat cardiac scans in list-mode with 16 ECG-gates with PET as well as FDG. The investigators suggested a custom coupled active contour framework for reducing contamination from blood to tissue as well as from tissue to blood that are because of organ movement as well as spillovers. The novel discoveries included the fact that the investigators appended external energies to internal contours for considering the contrast blood-to-tissue as significant as the contrast tissue-to-outside myocardium. For correcting blood as well as tissue areas for spillovers, the investigators disintegrated the two dynamic ROIs in the blood as well as tissue component through usage of Bayesian probability. The outcomes revealed an excellent distinction of blood as well as tissue component in images as opposed to external blood sampling.

Gray et al., [11] suggested the initial usage of multi-region FDG-PET information for classifying subjects from Alzheimer's Disease Neuroimaging Initiative. Image information was acquired from 69 normal subjects, 71 Alzheimer's afflicted individuals as well as 147 individuals with base diagnosis of mild cognitive impairment (MCI). Anatomical segmentation was automatically created in the native MRI-space of all subjects while the mean signal intensity per cubic millimetre in all regions were extricated from the FDG-PET scans. Through usage of FDG-PET, a method that is frequently utilized clinically in the workup of dementia patients, the investigators attained outcomes that are equivalent to those got through data from research-quality MRIs or biomarkers got in an invasive way from cerebrospinal fluid.

Zhenget al., [12] suggested a new model for the derivation of generalized optimum quantitative index (QI) as well as its related optimum range of imaging protocols for more enhancement of performance of dual-time FDG-PET imaging in diagnosing lung cancers.

Tafstet et al., [13] suggested a novel technique for segmenting (BTV) in <sup>18</sup>F-FDG-PET scans through usage of an automated Gaussian mixture model (GMM) on the basis of Akaike information criteria (AIC). The protocol was confirmed as valid on two patients out of seven who had laryngeal tumour. The volumes predicted were contrasted with macroscopic laryngeal specimens wherein a 3-D biological tumour volume (BTV) specified by histology was utilized as reference. Outcomes from experiments revealed that the technique was capable of segmenting BTV in a more accurate fashion than other threshold-based techniques.

## METHODOLOGY

### DATASET

A dataset comprising fifty one patients with histologically confirmed primary soft tissue sarcomas of the extremities was obtained in a retrospective fashion. Patients with metastatic and/or recurrent soft tissue sarcomas at presentation were discarded from the research. The individual were split into two broad groups [14]:

- 32 who did not develop lung metastases (represented as 'NoLungMets'); and
- 19 who developed lung metastases (represented as 'LungMets') within the follow-up period.

Individuals from the first with follow-up time lesser than a year were discarded from the research. Lung metastases were confirmed either through biopsies or through diagnoses by healthcare professionals through the presence of common pulmonary lesions in CT and/or FDG-PET scans.

### WAVELET

Features extraction is the initial phase of classification wherein features of all images are distinctly extricated from MRIs through wavelets which is regarded as the optimal technique for extracting most emphasizing pixels apparent in images for improving outcomes. For decomposition of data into distinct frequencies, wavelet mathematical functions are utilized and all components

are examined with resolutions matched to their degrees. For analyzing complicated dataset, wavelets are now regarded as the most powerful mathematical tool available.

Wavelet refers to mathematical functions that disintegrate data into distinct frequency components with resolutions matched as per its state. It has several advantages at the time of analysis of physical situations with discontinuities as well as sharp edges. Wavelet transforms are similar to hierarchical sub-band filtering systems. Mostly all practical DWTs utilize discrete time filter banks. These are known as wavelets as well as scaling coefficient in wavelet terminology.

Wavelet transforms (WT) are a comparatively novel kind of transform. A significant benefit is that the transform possesses the capacity to offer data regarding the time-frequency abstractions of the signal. For almost all practical applications, there are two types of wavelets present which are CWT as well as DWT. Wavelet coefficients at all scales generate large quantities of information. Because of the large quantities of information created via CWT, training classifiers on the basis of the coefficients at various scales may frequently become hard.

DWT refers to an implementation technique for wavelets following certain specified rules as well as discrete set of wavelet translations. It is required for practical computations to make wavelets discrete. Scale limits are then discredited with regard to translation limit ( $\tau$ ). The formula below reveals the scale as well as translation of wavelets:

$$s = 2^{-m}$$

$$\tau = n2^{-m}$$

The typical format of transform kind of image combination protocols is the wavelet fusion protocol due to its simplicity as well as its capacity to preserve time as well as frequency details of image scans to be combined. Wavelet transfers of wavelet fusion protocols of two registered scans  $P_1(x_1, x_2)$  and  $P_2(x_1, x_2)$ . It may be denoted by [15]:

$$I(x_1, x_2) = W^{-1}(\psi(W(P_1(x_1, x_2)), W(P_2(x_1, x_2))))$$

Wherein  $W$ ,  $W^{-1}$  as well as  $\psi$  represent wavelet transform operators, inverse wavelet transform operators as well as fusion rule, correspondingly.

### GREY LEVEL CO-OCCURRENCE MATRIXES (GLCM)

GLCM refers to a statistical technique of examination of textures which consider the spatial relations of pixels. GLCM function characterizes the texture of images through calculation of how frequently pairs of pixels with particular values as well as in particular spatial relation occur in a particular image. The features are created through calculation of features for all co-occurrence matrices acquired through the usage of directions  $0^\circ$ ,  $45^\circ$ ,  $90^\circ$ , and  $135^\circ$ , and then average of the four values.

The noted co-occurrence matrix features equation that calculated from image  $(i, j)$  are angular second moment, energy, contrast, dissimilarity as well as GLCM correlation.

$$ASM = \sum_{i,j=0}^{N-1} P_{i,j}^2$$

$$Energy = \sqrt{\sum_{i,j=0}^{N-1} P_{i,j}^2}$$

$$Contrast = \sum_{i,j=0}^{N-1} P_{i,j} (i-j)^2$$

$$Dissimilarity(DIS) = \sum_{i,j=0}^{N-1} P_{i,j} |i-j|$$

$$GLCM \text{ Correlation} = \sum_{i,j=0}^{N-1} P_{i,j} \left[ \frac{(i-\mu_i)(j-\mu_j)}{\sqrt{(\sigma_i^2)(\sigma_j^2)}} \right]$$

GLCM correlations indicate the linear dependency between

gray levels as well as neighbor pixels wherein  $\mu_i$  denotes horizontal mean in matrix,  $\mu_j$  denotes vertical mean in matrix,  $\sigma_i^2$  as well as  $\sigma_j^2$  denotes dispersion around the mean of combinations of target as well as neighboring pixel [16].

### CORRELATION-BASED FEATURE SELECTION (CFS)

Like most features selection protocols, CFS utilizes a search protocol alongside functions for evaluating merits of features subset. Heuristics through which CFS assesses excellent of features subset considers the utility of individual features for prediction of class labels along with level of inter-correlation amongst them.

Correlation coefficient is utilized for estimation of correlation between subsets of features as well as classes, and inter-correlations amongst features. Relevance of a set of attributes rises with correlation between attributes as well as classes, and reduces with increasing inter-correlation [17]. CFS is utilized for determining optimal features subset and is typically fused with search schemes like forward selection, backward elimination, bi-directional searches, best-first search as well as genetic search.

$$r_{zc} = \frac{k\bar{r}_{zi}}{\sqrt{k + k(k-1)\bar{r}_{ii}}}$$

where  $r_{z_i}$  refers to the correlation between summed features subset as well as the class parameter,  $k$  refers to the quantity of subset features,  $r_z$  refers to the average of correlations between the subset features as well as the class parameters, while  $r_i$  refers to the average inter-correlation between subset features.

### NEURAL NETWORK LANGUAGE MODEL (NNLM)

Neural Network (NN) is exhaustively utilized for patterns classification, because of the fact that they do not need any details about probability distributions as well as the a priori probabilities of various classes. Neural network classifications systems imitate the human approach to thinking and in particular scenarios, they provide the decision for several classes to indicate the possibility of few other infections. In the event of brain MRI classification as either normal or anomalous, the technique utilizes back propagation protocol LM with Artificial Neural Network (ANNLM) for categorizing inputs into the set of target categories (normal or anomalous) as per features extraction variables.

Levenberg-Marquardt (LM) strategy is a high order adaptive method and significantly reduces Mean Square Error of neural networks. In the suggested method, optimized LM strategy is employed for diminishing errors at the time of classification of tumours in brain MRIs. In the current study, MRIs are subjected to ANN strategy through LM training for discovering as well as categorizing occurrences of tumours in MRIs and experimental evaluation is carried out for deciding the sensitivity, specificity as well as accuracy of optimized LM strategy. The total procedure utilized in tumour in MRIs classification is given.

LM method as well as Network infrastructure,

Assume a nonlinear model of the generic form in MRI brain images classification,

$$x_i = p(y_i, \alpha) + \varepsilon_i \text{ where, } (i = 1, 2, 3, \dots, m) \text{ Wherein } \alpha \text{ refers to a vector comprising } n \text{ variables while } m > n.$$

It is also to be assumed that  $g$  is non-linear in  $\alpha^T = [\alpha_1, \alpha_2, \dots, \alpha_n]$ . The method of least squares is used for estimation of indefinite variables in the event of non-linear regression functions. Proportional to the strategy, estimates of  $\alpha_1, \alpha_2, \dots, \alpha_n$  are acquired through minimization of quantity,

$$\sum g_i^2(\alpha)$$

Sum of the squares of the errors of the estimations of the classification of normal or anomalous brain images is inferred through the previously mentioned, wherein:  $g_i(\alpha) = x_i - p(y_i, \alpha)$

As given by non-linear regressions, the strategy of non-linear least-squares data fitting possesses excellent form for gradient as well as Hessian.

Standard LM training procedure is given by the pseudo code below, [18]

- Initialize weights as well as variable  $\mu$  ( $\mu = .01$  is adequate).
- Calculate sum of squared errors over inputs  $F(w)$ .
- Solve (2) for obtaining increment of weights  $\Delta w$
- Recalculate sum of squared errors  $F(w)$

Utilizing  $w = w + \Delta w$  as the trial  $w$ , and assess

IF trial  $F(w) < F(w)$  in step 2 THEN

IF trial  $F(w) < F(w)$  in step 2 THEN

$$w = w + \Delta w$$

$$\mu = \mu \cdot \beta (\beta = .1)$$

Go back to step 2

ELSE

$$\mu = \mu / \beta$$

go back to step 4

END IF

### NEURAL NETWORK BACK PROPAGATION (NN\_BPP)

Neural networks comprise of sets of nodes as well as connections between them. Typically nodes are grouped in layers with connections that go from one layer to the next. Input layers of nodes are present that are activated by inputted image data. Output layers of nodes represent output classes to train for. There are one or more hidden layers in the middle. Nodes in a layer are linked to all nodes in the next. Nodes in hidden layers obtain inputs from all nodes in the earlier layer. Output values from hidden layers are spread to output layers which comprise one node for every output class. All node connections possess weights that

multiply the signal traversing the connection. Nodes in the hidden as well as output layers sum the weighted signals they obtain and employ functions for producing output values. During learning phases, example spectral pattern is passed through network in a set of iterations. The second stage in training is a backward pass through the network for reducing errors between the real as well as anticipated output.

Artificial neural networks (ANN) take into consideration classification as a significant research as well as application area. The primary shortcoming in utilizing ANN is the finding of accurate grouping of training, learning as well as transfer functions for classification of datasets with rising quantity of features as well as classified sets. The various combinations of functions as well as their impact when utilizing ANN as a classifier is examined and the accuracy of the functions are studied for several types of datasets. The real-life issues that are denoted by multi-dimensional data sets are obtained from medical backgrounds.

Classifying as well as clustering the datasets is important. Datasets are split into training as well as testing sets and have no utilization in the training procedure. The outcomes are got with the assistance of the data sets and are utilized for testing. Training sets are obtained from 2/3<sup>rd</sup> of the datasets and the remainder is taken up as test dataset. This is made via the measurement of accuracy attained through testing against the datasets. Then networks are simulated with the same information. Back propagation protocols train the neural networks. Gradient descent methods (GDM) were utilized for decreasing mean squared errors between network output as well as actual error rates. The variables given below are regarded for measuring efficacy of the network: rate of convergence, number of epochs for converging network, computed MSE.

With the adequate combinations of training, learning as well as transfer function, data set classification utilizes the very successful tool known as back propagation neural networks [19].

### STRUCTURE OPTIMIZED BINARY PARTICLE SWARM OPTIMIZATION (PSO)

Kennedy and Eberharts suggested a discrete binary variant of PSO for binary issues. Binary values may be representations of real values in binary search space. In bPSO, particles' personal bests as well as global bests are updated like in the continuous variant. The primary variation is that velocity of the particles is specified with regard to probabilities that a bit will modify to 1. Utilizing this definition, velocities are restricted to [0,1]. Hence maps are suggested for mapping all real valued numbers of velocity to [0,1]. Normalization functions utilized here are sigmoid functions given by:

$$v'_{ij}(t) = sig(v_{ij}(t)) = \frac{1}{1 + e^{-v_{ij}(t)}}$$

Furthermore the formula given above is utilized for updating velocity vectors of the particles. New positions of the particles are got through the formula given below:

$$x_{ij}(t+1) = \begin{cases} 1 & \text{if } r_{ij} < sig(v_{ij}(t+1)) \\ 0 & \text{otherwise} \end{cases}$$

Wherein  $r_{ij}$  refers to a uniform arbitrary number within [0,1] [20].

### RESULT AND DISCUSSION

The experiments conducted using 85 Normal, 35 sarcoma images from the dataset. [Figure -1 & 2] shows the sample images. [Table - 1] listed the experiment results.

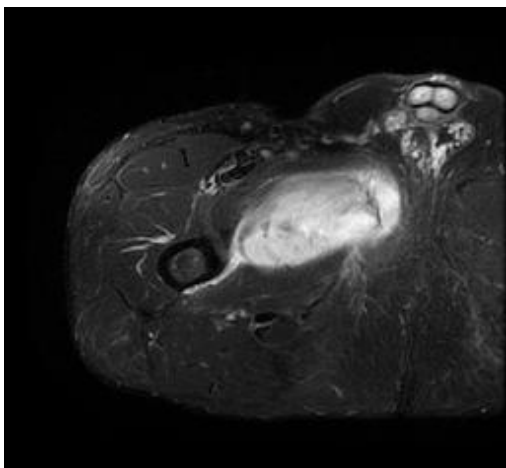


Fig: 1. Sample image 1

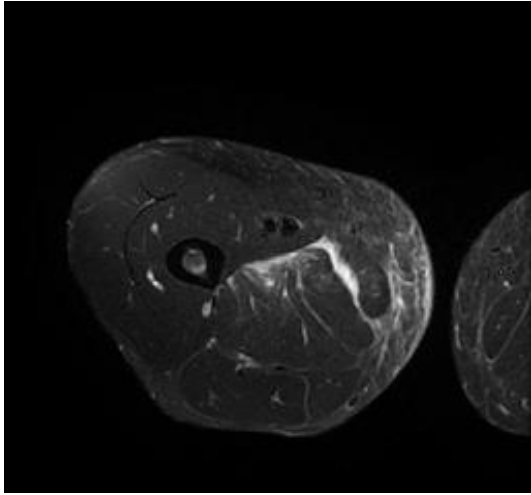


Fig: 2. Sample image 2

Table: 1. Results

Techniques	NN-BP	NN-LM	NN-structure optimized
classification accuracy	0.875	0.8898	0.925
Positive Prdictive Value for Normal	0.7632	0.8056	0.8421
Positive Prdictive Value for Bone Sarcoma	0.9268	0.9268	0.9634
Sensitivity for Normal	0.8286	0.8286	0.9143
Sensitivity for Bone Sarcoma	0.8941	0.9157	0.9294
F measure for Normal	0.9102	0.9212	0.9461
F measure for Bone Sarcoma	0.7946	0.8169	0.8767

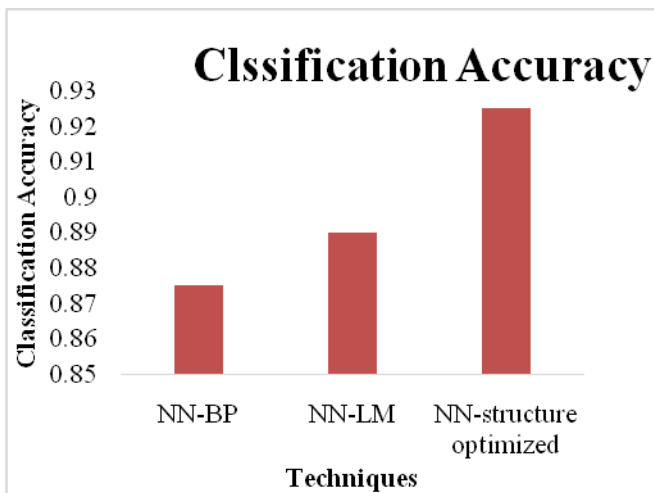
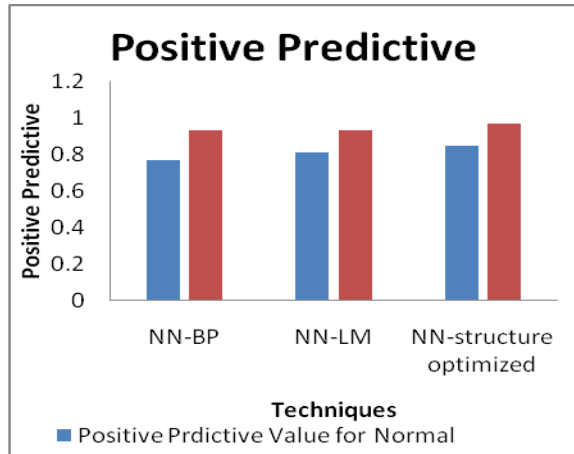


Fig: 3. Classification Accuracy

It can be observed from the [Figure -3] that the proposed NN-structure optimized with binary PSO method improved accuracy by 5.56% and 3.88% when compared with NN-BP and NN-LM approaches respectively.



**Fig: 4. Positive Predictive**

It can be observed from the [Figure -4] that the proposed NN-structure optimized with binary PSO method improved positive predictive value by 9.83% and 3.87% when compared with NN-BP for normal and bone sarcoma images respectively.

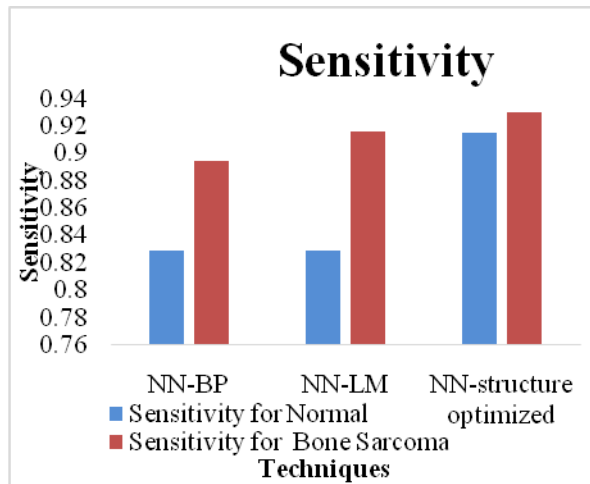


**Fig: 5. Sensitivity**

It can be observed from the [Figure -5] that the proposed NN-structure optimized with binary PSO method improved sensitivity value by 9.83% and 1.49% when compared with NN-LM for normal and bone sarcoma images respectively.

From [Figure -6] it is observed that the proposed NN-structure optimized with binary PSO method improved F measure value by 2.67% and 7.06% when compared with NN-LM for normal and bone sarcoma images respectively.

## CONCLUSION

STs typically form in the body's muscle, fat, nerve, deep skin tissue as well as blood vessels. Taken in tandem, FDG-PET definitely plays a growingly significant prognostic as well as predicting role in managing sarcoma. It can be utilized for assessing aggressiveness of tumours for making earlier clinical decision regarding the utility of treatment option for patients. In this paper, features extracted using wavelet and GLCM methods and CFS is used



for feature selection. And we proposed the neural network classifier optimized with the binary particle swarm optimization for the classification of sarcoma images. The results proved that the proposed optimization improved the accuracy, positive predictive and sensitivity as well as f measure.

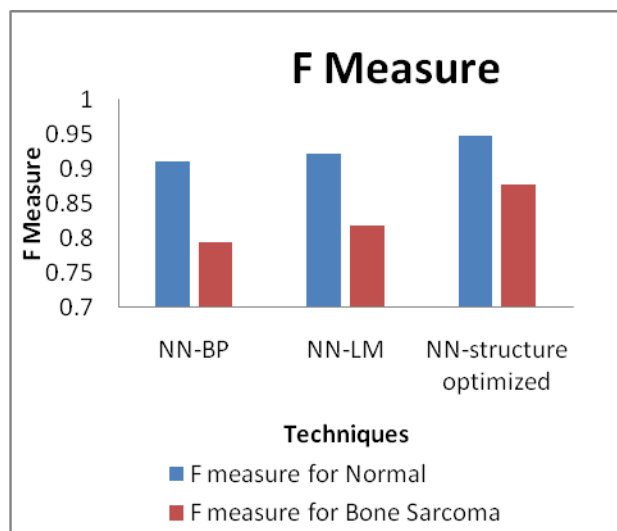


Fig: 6. F Measure

#### CONFLICT OF INTEREST

The authors declare no conflict of interests.

#### ACKNOWLEDGEMENT

None

#### FINANCIAL DISCLOSURE

The authors report no financial interests or potential conflicts of interest.

## REFERENCES

- [1] Levard A, Tassy L, Cassier PA. [2013] Emerging therapies for soft-tissue sarcomas. *Hematology/oncology clinics of North America*, 27(5): 1063-1078.
- [2] Mankin HJ, Hornicek FJ. [2005] Diagnosis, classification, and management of soft tissue sarcomas. *Cancer Control*, 12(1): 5-21.
- [3] Benz MR, Czernin J, Allen-Auerbach MS, Tap WD, Dry SM, Elashoff D, Weber WA. [2009] FDG-PET/CT imaging predicts histopathologic treatment responses after the initial cycle of neoadjuvant chemotherapy in high-grade soft-tissue sarcomas. *Clinical cancer research*, 15(8): 2856-2863.
- [4] Musana KA, Raja S, Cangelosi CJ, Lin YG. [2006] FDG PET scan in a primitive neuroectodermaltumor. *Annals of nuclear medicine*, 20(3): 221-225.
- [5] Farhidzadeh H, Goldgof DB, Hall LO, Gatenby RA, Gillies RJ, Raghavan M. [2015] Texture feature analysis to predict metastatic and necrotic soft tissue sarcomas.
- [6] Karakatsanis NA, Lodge MA, Zhou Y, Mhlanga J, Chaudhry MA, Tahari AK, Rahmim A. [2011] Dynamic multi-bed FDG PET imaging: feasibility and optimization. In *Nuclear Science Symposium and Medical Imaging Conference (NSS/MIC)*, IEEE (pp. 3863-3870).
- [7] O'Sullivan F, Wolsztynski E, O'Sullivan J, Richards T, Conrad EU, Eary JF. [2011] A statistical modeling approach to the analysis of spatial patterns of FDG-PET uptake in human sarcoma. *Medical Imaging, IEEE Transactions on*, 30(12):059-2071.
- [8] Wang J, Feng DD, Xia Y. [2010] Automated Detection of the Occurrence and Changes of Hot-Spots in Intro-subject FDG-PET Images from Combined PET-CT Scanners. In *Digital Image Computing: Techniques and Applications (DICTA)*, 2010 International Conference on, IEEE, (pp. 63-68).
- [9] Zhong M, Kundu BK. [2013] Optimization of a model corrected blood input function from dynamic FDG-PET

- images of small animal heart in vivo. *Nuclear Science, IEEE Transactions on*, 60(5):3417-3422.
- [10] Mabrouk R, Bentabet L, Dubeau F, Bentourkia M. [2010] Input functions extraction from gated 18 F-FDG PET images. In *Nuclear Science Symposium Conference Record (NSS/MIC)*, IEEE (pp. 2982-2986).
- [11] Gray KR, Wolz R, Keihaninejad S, Heckemann RA, Aljabar P, Hammers A, Rueckert D. [2011] Regional analysis of FDG-PET for use in the classification of Alzheimer's disease. In *Biomedical Imaging: From Nano to Macro, IEEE International Symposium on* (pp. 1082-1085). IEEE.
- [12] Zheng X, Tian G, Wen L, Feng DD. [2010] Generalized optimal quantitative index of dual-time FDG-PET imaging in lung cancer diagnosis. In *Biomedical Imaging: From Nano to Macro, 2010 IEEE International Symposium on*, 201-204).
- [13] Tafast A, Hadjili ML, Hafdaoui H, Bouakaz A, Benoudjit N. [2015] Automatic Gaussian Mixture Model (GMM) for segmenting 18 F-FDG-PET images based on Akaike Information Criteria.
- [14] Freeman C R, Skamene SR, El Naqa, I. [2015] A radiomics model from joint FDG-PET and MRI texture features for the prediction of lung metastases in soft-tissue sarcomas of the extremities. *Physics in medicine and biology*, 60(14):5471.
- [15] Korchiyne R, Farssi SM, Sbihi A, Touahni R, Alaoui MT. [2014] A Combined Method Of Fractal And GLCM Features For MRI And CT Scan Images Classification. arXiv preprint arXiv:1409.4559.
- [16] Kaur N, Bahl M, Kaur H, [2014] Review On: Image Fusion Using Wavelet and Curvelet Transform. *International Journal of Computer Science and Information Technologies*, 5 (2):2467-2470
- [17] Karegowda AG, Manjunath AS, Jayaram MA. [2010] Comparative study of attribute selection using gain ratio and correlation based feature selection. *International Journal of Information Technology and Knowledge Management*, 2(2):271-277.
- [18] Palanivelu L, Vivayakumar P. [2014] IMPROVED NEURAL NETWORK TRAINING ALGORITHM FOR CLASSIFICATION OF COMPRESSED AND UNCOMPRESSED IMAGES. *Journal of Theoretical & Applied Information Technology*, 62(1).
- [19] Saravanan K, Sasithra S. [2014] Review On Classification Based On Artificial Neural Networks. *International Journal of Ambient Systems and Applications (IJASA)* 2(4)
- [20] Khanesar MA, Teshnehlab M, Shoorehdeli MA. [2007] A novel binary particle swarm optimization. In *Control & Automation, 2007. MED'07. Mediterranean Conference on* (pp. 1-6). IEEE.

\*\*DISCLAIMER: This published version is uncorrected proof; plagiarisms and references are not checked by IIOABJ; the article is published as it is provided by author and approved by guest editor.